

# Different back electron transfer from titanium dioxide nanoparticles to tetra (4-sulfonatophenyl) porphyrin monomer and its J-aggregate

Xiujuan Yang, Zhifei Dai, Atsushi Miura, Naoto Tamai \*

*Department of Chemistry, School of Science, Kwansai Gakuin University, 1-1-155 Uegahara, Nishinomiya 662-8501, Japan*

Received 26 October 2000; in final form 4 December 2000

## Abstract

The synthesized titanium dioxide ( $\text{TiO}_2$ ) nanoparticle was found to enhance the formation of J-aggregate of water-soluble porphyrin, tetra (4-sulfonatophenyl) porphyrin dye, 5,10,15,20-tetraphenyl-21H, 23 H-porphine tetrasulfonic acid (TPPS). The forward and back electron transfers (ETs) between adsorbed TPPS and  $\text{TiO}_2$  nanoparticles were examined by picosecond single-photon timing and femtosecond transient absorption spectroscopy. The ultrafast back ET of  $\sim 0.8$  ps was observed both for the protonated monomer and the J-aggregate. The back ET almost completes within a few tens of picoseconds for the protonated monomer, while  $>1$  ns is required for the J-aggregate. The difference has been interpreted in terms the hole delocalization and electronic coupling of the protonated monomer and J-aggregate adsorbed on  $\text{TiO}_2$  nanoparticles. © 2001 Elsevier Science B.V. All rights reserved.

## 1. Introduction

Either as a photocatalyst for degradation of organic pollutants or solar energy conversion devices, interfacial electron transfer (ET) on titanium dioxide ( $\text{TiO}_2$ ) nanoparticles appears to be the main focus of most of these studies to investigate determining factors for high catalytic reactivity and electrical energy efficiency [1–6]. ET dynamics has been examined between different molecular adsorbates and  $\text{TiO}_2$  nanoparticles in numerous studies. With the report of solar to electrical energy conversion efficiency of  $\sim 10\%$  for ruthenium bipyridyl dye sensitized photovoltaic cell developed

by Grätzel and co-workers [5], various kinds of dyes were combined to  $\text{TiO}_2$  nanoparticles or thin films to investigate the mechanism of forward and back ETs [7–14].

In these studies, the dye molecules were excited using suitable optical wavelength, and consequent dynamics of forward electron injection within the excited-state lifetime of the dye was measured by transient absorption or fluorescence decays. On the other hand, the rate of back ET was also measured by monitoring the bleach recovery of the ground-state absorption of the dye [15]. Although the rates of back ET for various classes of dye molecules linked to  $\text{TiO}_2$  nanoparticles have been reported from a few picoseconds to milliseconds [7,15–20], details of the underlying reaction mechanism are still far from being understood. The injected electron from conduction band edge

\* Corresponding author. Fax: +81-798-51-0914.

E-mail address: tamai@kwansai.ac.jp (N. Tamai).

may undergo shallow and deep trap states, or directly go back to dye cation. Several recent studies have shown, in contrast to forward electron injection, the back ET is rather sensitive to experimental conditions such as solvent environments, external bias, types of adsorbates, size of nanoparticles, and so on [15,16]. Therefore, an effort is essentially necessary to make clear the understanding of the dependence of back ET kinetics on a single parameter.

Tetra (4-sulfonatophenyl) porphyrin dye, 5,10,15,20-tetraphenyl-21H, 23 H-porphine tetrasulfonic acid (TPPS) is a water-soluble porphyrin and its aggregate can be controlled by ionic strength or pH of the solution [21–23]. In the present work, we have examined the back ET kinetics of TPPS sensitized TiO<sub>2</sub> nanoparticles by femtosecond transient absorption spectroscopy. It was found that the aggregation is easily induced by the strong electrostatic interaction between the SO<sub>3</sub><sup>-</sup> group of the protonated TPPS monomer and the positively charged TiO<sub>2</sub> surface. Moreover, the co-adsorption of the protonated TPPS monomer and its J-aggregate allows us to compare their back ET kinetics from TiO<sub>2</sub> nanoparticles in the same colloidal system minimizing the difference of experimental conditions. The electron injection to nanoparticles has been confirmed by the steady-state fluorescence quenching and picosecond single-photon timing spectroscopy, whereas the dynamics of back ET has been probed by transient absorption from the ground-state bleaching recovery of the protonated monomer and its J-aggregate, respectively.

## 2. Experimental

### 2.1. Sample preparation

Nanosized colloidal TiO<sub>2</sub> particles were prepared by controlled hydrolysis of titanium (IV) tetraisopropoxide, Ti[OCH(CH<sub>3</sub>)<sub>2</sub>]<sub>4</sub>, in water under deaerated conditions with pure N<sub>2</sub> and controlled pH. A 5 ml aliquot of Ti[OCH(CH<sub>3</sub>)<sub>2</sub>]<sub>4</sub> dissolved in isopropyl alcohol (5:95) was added drop-wise to 900 ml of pure water with a resistivity of 18 MΩ cm (2°C) at pH = 2 adjusted with HNO<sub>3</sub>

[24]. After continuous stirring for 12 h or longer, the solution became transparent and TiO<sub>2</sub> nanoparticles formed. Following rotary evaporation at 30°C, a slightly yellowish crystal-like powder was obtained, which could be resuspended in pure water to obtain perfectly transparent colloidal TiO<sub>2</sub> suspension. The average diameter of the synthesized TiO<sub>2</sub> nanoparticles was estimated to be ~7 nm on a solid surface by AFM (Topometrix, Explorer). The observed particles probably include the aggregates of TiO<sub>2</sub>, so that the diameter of a particle in solution may be smaller than ~7 nm.

TPPS was used as purchased from Wako Pure Chemical Industries. An aqueous solution of  $1 \times 10^{-3}$  M TPPS was prepared prior to each measurement and was used to obtain the desired concentration by adding this solution to a certain amount of purified water. The sensitized TiO<sub>2</sub> colloidal solution was prepared by dissolving the desired amount of TiO<sub>2</sub> powder. The final pH of the solution was adjusted by dropping HCl solution. Steady-state absorption and fluorescence spectra were recorded with a U-3120 (Hitachi) spectrophotometer and a FluoroMax-2 (Jobin-Yvon SPEX) spectrofluorimeter, respectively.

### 2.2. Laser system

The back ET kinetics between TiO<sub>2</sub> nanoparticles and the adsorbed protonated TPPS monomer and its J-aggregate were measured with a regeneratively amplified Ti: sapphire laser system (Spectra-Physics, Tsunami and Spitfire). The excitation pulse at ~410 nm was taken from the second harmonics of an amplified fundamental laser beam at ~820 nm, while the probe beam used here was femtosecond white-light continuum that was generated by focusing the residual of the fundamental laser beam into a 1 cm H<sub>2</sub>O cell. The repetition rate of the excitation pulse was 1 kHz. The energy was adjusted to 3 μJ/pulse. The transient absorption signal was measured with a monochromator (Japan Spectroscopic, CT-10)–photodiode combination. The sample was flowed in a 2 mm thick cell driven by a peristaltic pump (Cole Parmer Instrument, Model 7090-42). Fluorescence decay dynamics was measured by a picosecond single-photon timing spectroscopic

system. Rise and decay curves of transient absorption and fluorescence were analyzed by a non-linear least-squares iterative convolution method based on a Marquardt algorithm.

### 3. Results and discussion

#### 3.1. Co-adsorption of protonated monomer and J-aggregate on TiO<sub>2</sub> nanoparticles

Fig. 1 illustrates the absorption spectra of aqueous solutions of TPPS with and without TiO<sub>2</sub> nanoparticles. TPPS exists as a protonated monomer in the concentration of  $1 \times 10^{-5}$  M at pH = 2.9 [21]. The solution exhibits absorption bands at 433 nm (Soret-band), and 593 nm and 644 nm (Q-bands) (Fig. 1a). By reducing the pH of the solution to 1, a new absorption band appears as shown in Fig. 1b, which is characterized by its sharp peak at 490 nm and a narrow bandwidth of 7 nm. This absorption spectrum can be safely assigned to the J-aggregate of TPPS [21–23].

After the addition of a small amount of TiO<sub>2</sub> nanoparticles to the protonated monomer solution

prepared at the concentration of  $2 \times 10^{-5}$  M and pH = 2.9, the absorption spectrum changed in both Soret- and Q-band regions as shown in Fig. 1c. The characteristic Soret-band peak of the protonated monomer moves to 427 nm with a blue shift of 6 nm, which indicates its adsorption on the surface of TiO<sub>2</sub> nanoparticles. In addition, a new absorption band at 481 nm was observed. This absorption is probably due to the TPPS J-aggregate adsorbed on TiO<sub>2</sub> nanoparticles. Comparing with that of the J-aggregate in aqueous solution (Fig. 1b), the 9 nm blue shift indicates a little change in the electronic structure of J-aggregate due to the electrostatic interaction between adsorbed TPPS and TiO<sub>2</sub> nanoparticles. The bandwidth of the adsorbed J-aggregate is broadened to 12 nm, which is another evidence for that the TPPS J-aggregate is formed when the protonated monomers are adsorbed on the surface of TiO<sub>2</sub> nanoparticles. We therefore conclude that TiO<sub>2</sub> nanoparticles can enhance the formation of TPPS J-aggregate leading to co-adsorption of the protonated monomer and the J-aggregate on the surface of nanoparticles.

#### 3.2. Forward electron injection

According to Gilman equation [25], the energy of the highest occupied level ( $E_{HO}$ ) and lowest vacant level ( $E_{LV}$ ) of a dye can be easily calculated from the oxidation or reduction potential. The calculated values of  $E_{LV}$  are  $-2.94$  and  $-2.92$  eV with respect to the vacuum level for the protonated monomer and the J-aggregate, respectively. These values are close to the reported data of  $E_{LV}$  for zinc porphyrin,  $-3.27$  eV, which has been demonstrated to be an efficient TiO<sub>2</sub> sensitizer [26]. In addition, these  $E_{LV}$  values are larger than the conduction band ( $E_{CB}$ ) of anatase TiO<sub>2</sub> ( $-4.26$  eV at pH = 3) [3,26,27]. Thus ET from the singlet excited states of both species to the conduction band of TiO<sub>2</sub> is thermodynamically allowed.

Fig. 2A illustrates the fluorescence spectra of the protonated monomer and the J-aggregate in aqueous solution. The characteristic fluorescence peaks are located at 672 and 715 nm for the protonated monomer and the J-aggregate, respectively. By adding TiO<sub>2</sub> nanoparticles into

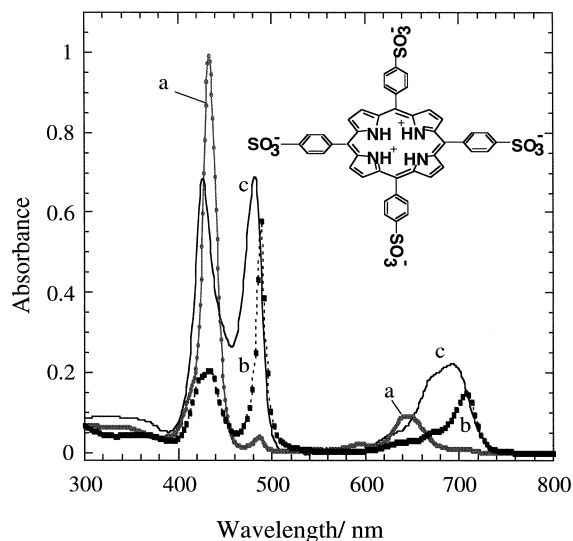


Fig. 1. Absorption spectra of (a) 10  $\mu$ M TPPS in aqueous solution at pH = 2.9, (b) 10  $\mu$ M TPPS in aqueous solution at pH = 1.0, and (c) 20  $\mu$ M TPPS aqueous solution with 4 g/l TiO<sub>2</sub>, at pH = 2.9.

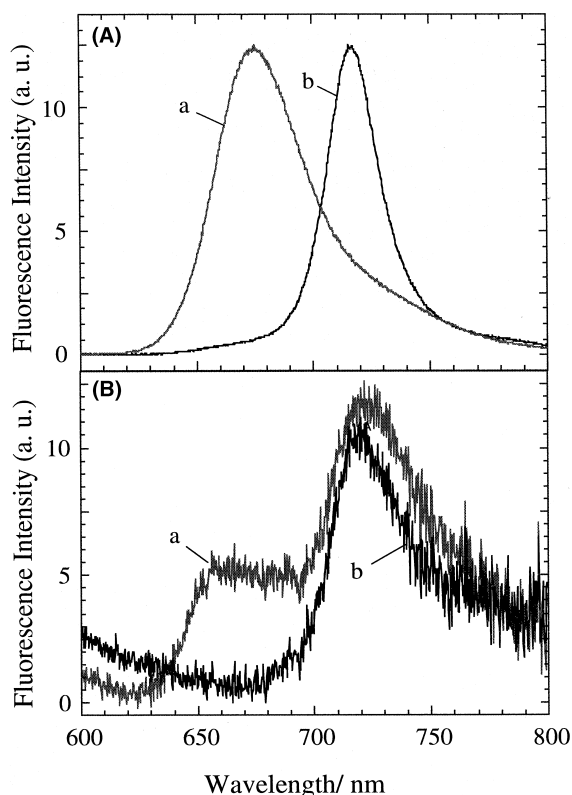


Fig. 2. (A) Fluorescence spectra of 10  $\mu\text{M}$  TPPS aqueous solution without  $\text{TiO}_2$ : (a) at  $\text{pH} = 2.9$  with the excitation wavelength of 430 nm, and (b) at  $\text{pH} = 1.0$  with the excitation wavelength of 488 nm. (B) Fluorescence spectra of 20  $\mu\text{M}$  TPPS aqueous solution with 4 g/l  $\text{TiO}_2$  at  $\text{pH} = 2.9$  with the excitation wavelength (a) at 430 nm and (b) at 480 nm.

TPPS solution, the fluorescence of both species is considerably quenched as shown in Fig. 2B. The quenched fluorescence has a peak at  $\sim 660$  nm for the protonated monomer and at  $\sim 715$  nm for the J-aggregate on  $\text{TiO}_2$  nanoparticles. The quenching ratios ( $\eta = I/I_0$ ,  $I$  and  $I_0$  are the integrated fluorescence intensities of TPPS with and without  $\text{TiO}_2$  nanoparticles) of the protonated monomer and the J-aggregate were examined by selecting the excitation wavelength in respective Soret band and taking the absorbance for each case into account.  $\eta$  values were estimated to  $\sim 4.8 \times 10^{-5}$  for the protonated monomer and  $\sim 1.4 \times 10^{-3}$  for the J-aggregate. These results suggest that when the protonated monomer and the J-aggregate are adsorbed on  $\text{TiO}_2$  nanoparticles, both of them can

efficiently inject an electron into  $\text{TiO}_2$  conduction band from their excited singlet states, although the quenching efficiency is higher for the protonated monomer than the case for J-aggregate.

Fig. 3 illustrates the fluorescence decay dynamics of the protonated monomer in solution (Fig. 3A) and TPPS adsorbed on  $\text{TiO}_2$  nanoparticles (Fig. 3B). The best fit for the protonated monomer in solution shows a single exponential decay with a lifetime of 3.95 ns, which is in good agreement with the reported lifetime (3.9 ns) [22,28]. For the TPPS adsorbed on  $\text{TiO}_2$  nano-

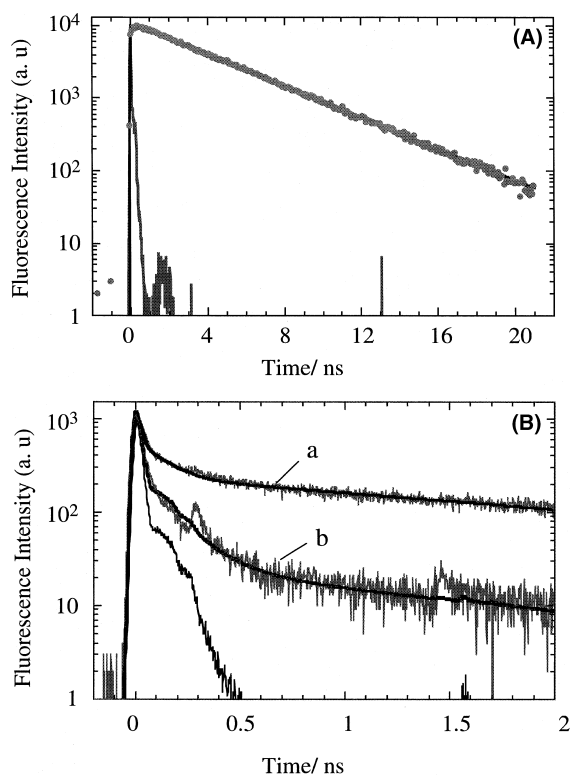


Fig. 3. (A) A fluorescence decay curve of protonated TPPS monomer in aqueous solution excited at 527 nm and observed at 660 nm. The lifetime was analyzed to be 3.95 ns. (B) Fluorescence decay curves of TPPS adsorbed on  $\text{TiO}_2$  nanoparticles (4 g/l  $\text{TiO}_2$ ) at  $\text{pH} = 2.9$ . The sample was excited at 410 nm and the fluorescence decays were observed at 660 nm (a) and 715 nm (b). The lifetimes for the adsorbed protonated monomer were  $< 2$  ps (96.4%), 71 ps (2.6%), and 2.4 ns (1.0%) for the decay (a). The lifetimes of the adsorbed J-aggregate were analyzed to be  $< 2$  ps (99.6%), 156 ps (0.3%), and 1.8 ns (0.1%) for the decay (b).

particles, a non-exponential fluorescence behavior with an ultrafast decay component was observed for both the protonated monomer and the J-aggregate. The fluorescence decay of the protonated monomer adsorbed on TiO<sub>2</sub> nanoparticles at 660 nm was analyzed by a sum of three-exponential decay function with lifetimes of <2 ps (96.4%), 71 ps (2.6%), and 2.4 ns (1.0%). On the other hand, the lifetimes of the J-aggregate adsorbed on TiO<sub>2</sub> nanoparticles were analyzed to be <2 ps (99.6%), 156 ps (0.3%), and a negligible long decay component of 1.8 ns (0.1%). The lifetime of the J-aggregate in aqueous solution has been reported to be ~50 ps [23], which is much longer than the main component (<2 ps) for the J-aggregate adsorbed on TiO<sub>2</sub> nanoparticles. The fastest decay component is limited by a temporal resolution of our single-photon timing system, indicating the presence of electron injection process shorter than 2 ps from the protonated monomer and the J-aggregate into TiO<sub>2</sub> nanoparticles.

By comparing the steady-state quenching ratio and the fluorescence dynamics, the quenching efficiency of the protonated monomer calculated from the steady-state experiments is ~150 times larger than that from the dynamic experiment. In the case of J-aggregate, the quenching efficiency is ~30 times larger in steady-state experiment than that in the dynamic experiment. This result suggests that an ultrafast electron injection process similar to the static quenching, which cannot be detected by single photon timing spectroscopy, exists in TPPS sensitized TiO<sub>2</sub> nanoparticles.

### 3.3. Back electron transfer

Co-adsorption of the protonated monomer and the J-aggregate on the TiO<sub>2</sub> nanoparticles minimizes the effect of different pH values and different surface properties of TiO<sub>2</sub> originated from the sample preparations, which allows us to compare the interfacial back ET kinetics between these two adsorbates with identical circumstance. When the TPPS modified TiO<sub>2</sub> nanoparticles were excited at 410 nm, two negative absorption bands were observed around 430 and 480 nm corresponding to the ground-state bleaching of the protonated monomer and the J-aggregate, respectively.

Fig. 4a illustrates the ground state bleaching at 430 nm of the protonated monomer in solution without TiO<sub>2</sub>. The bleaching recovery consists of a short-lived component of ~2.0 ps (23.8%) and a long lived component with the lifetime longer than 1 ns (76.2%). The long decay component corresponds to the lifetime of S<sub>1</sub> state, and the short one is probably due to the relaxation from the S<sub>2</sub> state. The lifetime of the fast decay is a little longer than the fluorescence lifetime of the S<sub>2</sub> state of protonated monomer (~600 fs) measured in our previous fluorescence up-conversion study [29]. The

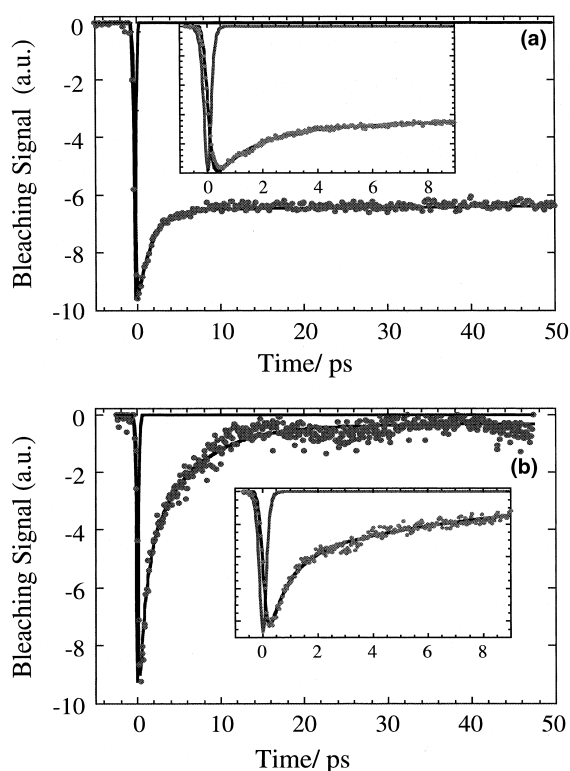


Fig. 4. (a) The dynamics of ground-state bleaching recovery of the protonated TPPS monomer in aqueous solution of pH = 2.9 observed at 430 nm. The insertion figure is the dynamics up to 8 ps. The lifetime of the recovery was analyzed to be 2.0 ps (23.8%) and >1 ns (76.2%). (b) The dynamics of ground-state bleaching recovery of the adsorbed protonated monomer on TiO<sub>2</sub> nanoparticles observed at 430 nm. The solution has 4 g/l TiO<sub>2</sub> at pH = 2.9. The insertion figure is the dynamics up to 8 ps. The lifetime of the recovery was analyzed to be 0.8 ps (52.5%), 5.6 ps (45.0%), and a few hundreds of ps to > ns (2.5%).

slow recovery of the ground-state absorption as compared with the fluorescence is probably due to the formation of vibrationally hot ground-state by the non-radiative relaxation from the  $S_2$  state. A further relaxation is required for thermally relaxed ground state, which results in the slow relaxation time in the ground-state bleaching recovery as compared with the fluorescence up-conversion.

In contrast to the dynamics in aqueous solution, a completely different behavior in the bleaching recovery was observed for TPPS sensitized  $\text{TiO}_2$  nanoparticles. Fig. 4b shows the ground-state recovery of the adsorbed protonated monomer at 430 nm. The decay curve fitting requires three time constants of 0.8 ps (52.5%), 5.6 ps (45.0%), and a few hundreds of ps to >ns (2.5%). The bleaching signal almost recovers within a few tens of ps, although the long component that cannot be determined well in our data exists to a little extent. It has been reported that the back ET is as fast as 1 ~ 2 ps (40 ~ 50%) in addition to a few tens of ps, a few hundreds of ps, and > ns components for  $\text{TiO}_2$  nanoparticles sensitized with  $\text{Fe}^{\text{II}}(\text{CN})_6^{4-}$  by the analysis of the ground-state bleaching recovery [15]. This result suggests that ~1 ps and ~6 ps components for the protonated monomer adsorbed on  $\text{TiO}_2$  nanoparticles are probably due to the back ET. The multi-exponential behavior is considered to be due to the distribution of shallow and deep trapping sites inside the  $\text{TiO}_2$  nanoparticles [31–34]. The fastest component may correspond to the back ET from surface states irrespective of the kind of adsorbates [15,30].

The decay kinetics of the bleaching recovery of TPPS J-aggregate in aqueous solution and adsorbed on  $\text{TiO}_2$  nanoparticles are given in Fig. 5. For making a critical comparison, the TPPS modified  $\text{TiO}_2$  colloidal solution used here is as the same as the monomer case except the observed wavelength at 480 nm corresponding to the bleaching band of the J-aggregate. Considerable care was taken during the measurements to make sure the equivalent experimental condition. The trace measured in Fig. 5a for the free J-aggregate shows two-exponential decay with the time constants of 1.5 ps (53.4%) and 52 ps (46.6%), in

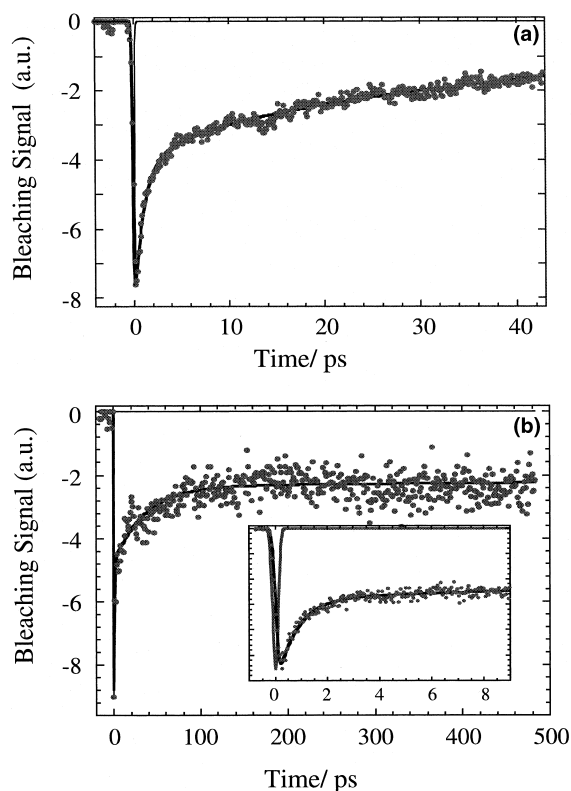


Fig. 5. (a) The dynamics of ground-state bleaching recovery of the TPPS J-aggregate in aqueous solution of pH = 1.0 observed at 480 nm. The lifetime of the recovery was analyzed to be 1.5 ps (53.4%) and 52 ps (46.6%). (b) The dynamics of ground-state bleaching recovery of the adsorbed TPPS J-aggregate on  $\text{TiO}_2$  nanoparticles observed at 480 nm. The solution has 4 g/l  $\text{TiO}_2$  at pH = 2.9. The insertion figure is the dynamics up to 8 ps. The lifetime of the recovery was analyzed to be 780 fs (71.6%), 42 ps (13.8%), and >1 ns (14.6%).

which the long lifetime is consistent with the reported lifetime of the J-aggregate [22]. The fast component is longer than the fluorescence lifetime of the  $S_2$  state of J-aggregate (~140 fs) measured in our previous fluorescence up-conversion study [29]. This behavior is similar to that of the protonated monomer as discussed above, and is probably explained in terms of the formation of vibrationally hot ground state by the non-radiative relaxation from the  $S_2$  state.

The decay curve of the ground state bleaching recovery of the J-aggregate adsorbed on  $\text{TiO}_2$  nanoparticles was illustrated in Fig. 5b. The dy-

namics corresponding to the interfacial back ET from TiO<sub>2</sub> to the J-aggregate displays a multi-exponential process with three time constants of 780 fs (71.6%), 42 ps (13.8%), and >1 ns (14.6%). A remarkably long component is observed for the adsorbed J-aggregate comparing with that for free J-aggregate, the behavior of which is completely different from that of the protonated monomer. On the other hand, the ultrafast back ET exists for the adsorbed J-aggregate as similar to the protonated monomer on TiO<sub>2</sub> nanoparticles, suggesting the role of surface states on the back ET.

The pronounced difference in the rate of back ET process between the protonated monomer and the J-aggregate adsorbed on TiO<sub>2</sub> nanoparticles indicates that the structures of adsorbed TPPS play an important role. Weng et al. [15] have suggested that the recombination kinetics are strongly dependent on the distance between electron trapped sites and adsorbates. After the excitation of the adsorbed protonated monomer and its J-aggregate, the hole is created in both adsorbed protonated monomer and J-aggregate following the electron injection. For the adsorbed J-aggregate, as a matter of positive carrier, the hole can be delocalized in a relatively large area of the aggregate, and even can diffuse along the J-aggregate chain to a certain extent. Moreover, the negative charge accumulated from a number of SO<sub>3</sub><sup>-</sup> groups may also neutralize the positive charge to some extent. All of these factors mentioned above, therefore, inhibit the electron recombination in the J-aggregate adsorbed on TiO<sub>2</sub> nanoparticles. In contrast to the J-aggregate, the diffusion distance of created hole in the protonated monomer is limited by only the size of a few Angstrom within the macrocycle. In addition, the size of the protonated monomer is rather small as compared with that of the J-aggregate, so that the monomer can approach to the surface of TiO<sub>2</sub> as close as possible, which could thereby strengthen the electronic coupling between the protonated monomer and TiO<sub>2</sub>. For the reduction of the rate of back ET in dye sensitized TiO<sub>2</sub> nanoparticle systems, the adsorbed J-aggregate is considerably suitable than the adsorbed protonated monomer.

#### 4. Summary

It was found that when the protonated TPPS monomer is adsorbed on TiO<sub>2</sub> nanoparticles, some of them form the J-aggregate. The co-adsorption of the protonated TPPS monomer and its J-aggregate on TiO<sub>2</sub> nanoparticles can minimize the environmental difference for the spectroscopic measurements. The steady-state fluorescence and picosecond single-photon timing spectroscopic measurements indicated that both adsorbed protonated monomer and J-aggregate can inject electron into TiO<sub>2</sub> conduction band from their excited singlet states. The interfacial back ET from TiO<sub>2</sub> to the protonated monomer and the J-aggregate was revealed to show multi-exponential kinetics by monitoring the ground-state bleaching recovery. The ultrafast back ET with a time constant of ~0.8 ps was observed for both the protonated monomer and the J-aggregate adsorbed on TiO<sub>2</sub> nanoparticles. The back ET almost completes within a few tens of ps for the adsorbed protonated monomer, while >1 ns is required for the adsorbed J-aggregate. The difference can be interpreted in terms of the difference of hole delocalization and electronic coupling of the protonated monomer and J-aggregate adsorbed on TiO<sub>2</sub> nanoparticles, in turns, to their different structures.

#### Acknowledgements

We would like to thank Prof. Tianhong Lu, Changchun Institute of Applied Chemistry, for valuable discussions. This work was partially supported by Grant-in-Aid for Scientific Research on Priority Area of 'Electrochemistry of Ordered Interface' (No. 10131266) from the Ministry of Education, Science, Sports and Culture, Japan.

#### References

- [1] P.V. Kamat, Chem. Rev. 93 (1993) 267.
- [2] M.A. Fox, M.T. Dulay, Chem. Rev. 93 (1993) 341.
- [3] A. Hagfeldt, M. Grätzel, Chem. Rev. 95 (1995) 49.
- [4] M.R. Hoffmann, S.T. Martin, W. Choi, D.W. Bahnemann, Chem. Rev. 95 (1995) 69.
- [5] B. O'Regan, M. Grätzel, Nature 353 (1991) 737.

- [6] G.J. Meyer, P.C. Searson, *Interface* 2 (1993) 23.
- [7] J.E. Moser, M. Grätzel, *Chem. Phys.* 176 (1993) 493.
- [8] S.G. Yan, J.T. Hupp, *J. Phys. Chem.* 100 (1996) 6867.
- [9] M. Hilgendorff, V. Sundström, *J. Phys. Chem. B* (1998) 10505.
- [10] S.A. Haque, Y. Tachibana, R.L. Willis, J.E. Moser, M. Grätzel, D.R. Klug, J.R. Durrant, *J. Phys. Chem. B* 104 (2000) 538.
- [11] Y. Wang, J.B. Asbury, T. Lian, *J. Phys. Chem. A* 104 (2000) 4291.
- [12] I. Martini, J.H. Hodak, G.V. Hartland, *J. Phys. Chem. B* 102 (1998) 9508.
- [13] A.C. Khazraji, S. Hotchandani, S. Das, P.V. Kamat, *J. Phys. Chem. B* 103 (1999) 4693.
- [14] A. Kay, R. Humphry-Baker, M. Grätzel, *J. Chem. Phys.* 98 (1994) 952.
- [15] Y. Weng, Y. Wang, J.B. Asbury, H.N. Ghosh, T. Lian, *J. Phys. Chem. B* 104 (2000) 93.
- [16] Y. Tachibana, H.A. Haque, I.P. Mercer, J.R. Durrant, D.R. Klug, *J. Phys. Chem. B* 104 (2000) 1198.
- [17] H.N. Ghosh, *J. Phys. Chem. B* 103 (1999) 10382.
- [18] I. Martini, J.H. Hodak, G.V. Hartland, P.V. Kamat, *J. Phys. Chem.* 107 (1997) 8064.
- [19] I. Martini, J.H. Hodak, G.V. Hartland, *J. Phys. Chem. B* 103 (1999) 9104.
- [20] I. Martini, J.H. Hodak, G.V. Hartland, *J. Phys. Chem. B* 102 (1998) 607.
- [21] O. Ohno, Y. Kaizu, H. Kobayashi, *J. Chem. Phys.* 99 (1993) 4128.
- [22] N.C. Maiti, M. Ravikanth, S. Mazmdar, N. Periasamy, *J. Phys. Chem.* 99 (1995) 17192.
- [23] N.C. Maiti, S. Mazmdar, N. Periasamy, *J. Phys. Chem. B* 102 (1998) 1582.
- [24] D. Bahnemann, A. Henglein, A.J. Lilie, L. Spanhel, *J. Phys. Chem.* 88 (1984) 709.
- [25] P.B. Gilman Jr., *Photogr. Sci. Eng.* 18 (1974) 475.
- [26] K. Kalyanasundaram, N. Vlachopoulos, V. Krishnan, A. Monnier, M. Grätzel, *J. Phys. Chem.* 91 (1987) 2342.
- [27] J. Xiang, C. Chen, B. Zhou, G. Xu, *Chem. Phys. Lett.* 315 (1999) 371.
- [28] D.L. Akins, J-aggregates, in: T. Kobayashi (Ed.), *World Scientific*, Singapore, 1996, pp. 67–94.
- [29] A. Miura, N. Tamai, H. Chosrowjan, Y. Shibata, N. Mataga, *Chem. Phys. Lett.*, submitted.
- [30] B.A. John, R.J. Ellingson, H.N. Ghosh, S. Ferrere, A.J. Nozik, T. Lian, *J. Phys. Chem.* 103 (1999) 3110.
- [31] G. Rothenberger, J. Moser, M. Grätzel, N. Serpone, D.K. Sharma, *J. Am. Chem. Soc.* 107 (1995) 8054.
- [32] D.P. Colombo Jr., K.A. Roussel, J. Saeh, D.E. Skinner, J.J. Cavaleri, R.M. Bowman, *Chem. Phys. Lett.* 232 (1995) 207.
- [33] D.P. Colombo Jr., R.M. Bowman, *J. Phys. Chem.* 100 (1995) 11752.
- [34] D.E. Skinner, D.P. Colombo Jr., *J. Phys. Chem.* 99 (1995) 7853.